



# Annatto (*Bixa orellana* L.), a potential novel starch source: antioxidant, microstructural, functional, and digestibility properties

Vianney Cortés-Viguri<sup>1</sup> · Landy Hernández-Rodríguez<sup>2</sup> · Consuelo Lobato-Calleros<sup>2</sup> · Juan C. Cuevas-Bernardino<sup>3</sup> · Blanca Elizabeth Hernández-Rodríguez<sup>2</sup> · Jose Alvarez-Ramirez<sup>4</sup> · E. Jaime Vernon-Carter<sup>4</sup>

Received: 9 September 2021 / Accepted: 8 October 2021 / Published online: 24 November 2021  
© The Author(s), under exclusive licence to Springer Science+Business Media, LLC, part of Springer Nature 2021

## Abstract

Bixin and norbixin are extracted from annatto seeds, and the residual seed waste can be used as a potential source of annatto starch (AS), contributing to the circular economy of the regional communities where the resource is grown/processed. To assess AS suitability as a food ingredient, its physicochemical, antioxidant, microstructural, and functional properties were evaluated after being purified by: Soaking in sodium metabisulfite solution (low purity), defatting for removing lipids (medium purity), alkaline treatment for extracting protein (medium purity), and combined defatting/alkaline (high purity) treatments. AS degree of purity affected all the evaluated parameters. The  $\zeta$ -potential values ranged between  $-18.30$  and  $-24.10$  mV and those of the antioxidant activity between  $0.52$  and  $1.14$   $\mu\text{g TE/g}$  (ABTS<sup>•+</sup> assay). AS presented a heterogeneous morphology with granules tending to agglomerate, and the mean Sauter diameter varied from  $26.8$  to  $31.1$   $\mu\text{m}$ . FTIR spectroscopy showed that protein molecules were present despite the alkaline treatment. X-ray patterns pinpointed that the starch crystalline region was not modified by the deproteinization treatment. The apparent viscosity and viscoelastic properties of gelatinized starch dispersions increased when lipids and proteins were simultaneously removed. The swelling power ( $21.44$ – $22.71$  g/g), solubility index ( $21.77$ – $40.43\%$ ), water absorption ( $3.9$ – $4.56$  g/g), and oil absorption ( $1.78$ – $2.41$  g/g) increased with the purification degree. The in vitro digestibility assay showed that AS presented a higher fraction of slowly digestible starch ( $36.57$ – $40.68\%$ ) than rapidly digestible and resistant starch fractions. This work demonstrates that AS has suitable functional properties that open the possibility for its use in the food industry.

**Keywords** Annatto starch · Digestibility · Functional properties · Purification treatments

## Abbreviations

AS	Annatto starch
$D_{3,2}$	Sauter mean diameter
OAC	Oil absorption capacity
RDS	Rapidly digestible starch
SDS	Slowly digestible starch
SI	Solubility index
SP	Swelling power
WAC	Water absorption capacity

✉ Landy Hernández-Rodríguez  
landy14hr@yahoo.com.mx; lhernandezr@chapingo.mx

<sup>1</sup> Posgrado en Ciencia y Tecnología Agroalimentaria, Departamento de Ingeniería Agroindustrial, Universidad Autónoma Chapingo, Km. 38.5 Carretera México-Texcoco, 56230 Texcoco, México

<sup>2</sup> Departamento de Preparatoria Agrícola, Universidad Autónoma Chapingo, Km 38.5 Carretera México-Texcoco, 56230 Texcoco, México

<sup>3</sup> CONACYT – Centro de Investigación y Asistencia en Tecnología y Diseño del Estado de Jalisco, A.C., Subsele Sureste, Parque Científico Tecnológico de Yucatán, km 5.5. Carretera Sierra Papacal - Chuburná Puerto, 97302 Mérida, Yucatán, México

<sup>4</sup> Departamento de Ingeniería de Procesos e Hidráulica, Universidad Autónoma Metropolitana-Iztapalapa, Iztapalapa, 09340 Mexico City, México

## Introduction

Annatto (*Bixa orellana* L.) is a native plant from America, whose economic and commercial importance lies in extracting natural pigments (bixin and norbixin) from its seeds. These pigments are widely employed as a condiment in traditional Mexican cuisine. They are also used in industrial applications for coloring processed foods (mainly dairy

products), oils, paints, cosmetics, and textile fibers [1]. Also, several studies have pinpointed that annatto seeds are sources of tocotrienols and phenolic compounds with beneficial biological properties. Extracts obtained from annatto leaves and seeds have shown antibacterial, antifungal, antioxidant, antidiarrheal, anticonvulsant, and analgesic capabilities [2–4].

Regardless of the pigment extraction process used in annatto seeds, by-products accounting for around 97 to 98% (dry weight) of the seeds are generated [5, 6]. The extracted seed wastes contain 40–75% (w/w) of carbohydrates, of which approximately 19 to 30% (w/w) is starch [5, 6]. Starch with various purity degrees can be obtained from the annatto residues depending on the extraction and depigmentation method employed [7, 8]. It is known that the presence of proteins, lipids, and other carbohydrates modify the thermal, rheological, pasting, and digestibility properties of different starch sources. For example, lipid and protein removal in rice and adlay seed starches caused a decrease in thermal stability but increased digestibility, relative crystallinity, and peak viscosity [9, 10]. In general, protein content is removed from the starch granule to enhance its functional properties. Several methods have been proposed for protein depletion, like enzymatic and chemical treatments. In the latter case, the use of aqueous NaOH solutions is most common. Alkali concentration, soaking time, and temperature can change the structure and functionality of the starch granules [11, 12]. Studies conducted with potato, sago, and corn starches have shown an increase in swelling power, solubility, and syneresis values after being treated under different NaOH concentrations for protein depletion [13, 14]. In this context, the importance of investigating the starch changes related to the presence or absence of native lipids and proteins is evident. The broad utility of starches in the food industry depends on their ability to modify the viscoelastic, culinary, and sensory properties of processed foods [15, 16].

Some studies have shown that starches obtained from non-conventional sources have antioxidant activity, distinguishing them from conventional starches [7, 17, 18]. It has been shown that annatto seeds have a high content of antioxidant compounds [1]. Therefore, it is of interest to identify whether the starch obtained from the seeds preserves phenolic compounds with antioxidant activity. Several works have focused on the morphological, thermal, and pasting properties of annatto starch [7, 8], but none on its functional properties (e.g., swelling power, solubility, and absorption capacity) and *in vitro* digestibility.

This study aimed to evaluate the physicochemical (particle size, rheology), phenolic content and antioxidant activity, microstructural (scanning electron microscopy, FTIR, XRD), functional properties (swelling, solubility, water, and oil absorption), and the *in vitro* digestibility of annatto starch, as influenced by different purification methods. It is

hoped that this study may promote the use of annatto starch for specific applications in the food industry.

## Material and methods

### Materials

Annatto seeds (*Bixa orellana* L.) were acquired in September 2018 at a local market in San Sebastian Yaxche, Peto, Yucatan, Mexico (GPS coordinates of 19°58'53" N and 88°55'28" W, elevation above sea level of 42 m). The seeds were stored in airtight plastic bags at 5 °C until required for their use. Gallic acid (G7384), 2,2-azino-bis-(3-ethylbenzothiazoline-6-sulfonic acid) diammonium salt (ABTS, A1888), 6-hydroxy-2,5,7,8-tetramethylchroman-2-carboxylic acid (Trolox, 238813), 2,20-diphenyl-1-picrylhydrazyl (DPPH, D9132), pancreatin from porcine pancreas (P1750), amyloglucosidase (A7095, EC 3.2.1.3), invertase (I4504, EC 3.2.1.26), and glucose oxidase–peroxidase reagent (GAGO20) were purchased from Sigma-Aldrich (St. Louis, MO, USA). All other chemical reagents were of analytical grade, and distilled water was used.

### Starch extraction

Annatto seeds (100 g) were twice depigmented with 300 mL of 2% (w/v) KOH for 12 h and 45 min, respectively, with constant stirring. The colored solutions were separated in each case [19]. The vegetal residue was dried at 50 °C for 24 h using a forced ventilation oven (HCF-S2-D, Riessa Digital, Mexico City, Mexico), milled with a commercial blender, sieved (20-mesh) until obtaining a fine flour. The annatto flour (AF) was subjected to four procedures to obtain different starch purities (see Supplementary Material—Fig. S1): A low purity starch ( $AS_L$ ) was obtained by soaking AF (100 g) with a 0.5% (w/v) sodium metabisulfite solution ( $Na_2S_2O_5$ ) (1:10, w/v ratio) [8]. The obtained starch was dried (45 °C for 20 h), ground (pestle and mortar), and passed through an 80-mesh sieve. Two medium purity starches were extracted by a defatting ( $AS_{F0}$ ) and by alkaline treatment to remove soluble proteins ( $AS_{P0}$ ). For  $AS_{F0}$ , the AF was defatted in a Soxhlet apparatus with petroleum ether for 5 h previous to the starch extraction [10]. For  $AS_{P0}$ , 50 g of  $AS_L$  was soaked in 100 mM NaOH solution at 30 °C (1:10, w/v ratio) with magnetic stirring for 4 h and resting for 44 h. The sediment was washed five times with distilled water, and the pH was adjusted to 7.0 [20]. The resulting starch was washed three times with 96% ethanol, dried and milled at the conditions mentioned before. A high purity starch ( $AS_{F0P0}$ ) was obtained by AF defatting followed by starch extraction and subsequent alkaline deproteinization with NaOH solution.

The extraction yield was calculated as the amount of obtained starch from 100 g of AF (dry basis) in each treatment [7].

### Proximal chemical composition

The moisture, protein, ash, lipid, and crude fiber contents in the annatto starches (AS) were determined by the AACC methods 44–15.02, 46–13, 08–17.01, 30–25.01, and 32–10.01, respectively [21]. Total carbohydrates were calculated by difference. The results of chemical composition were expressed on a dry basis (db). The apparent amylose content was estimated by the dual-wavelength iodine binding technique [22]. AS sample (100 mg, db) was mixed with 1 mL of ethanol and 10 mL of NaOH (1 N) into a 100 mL volumetric flask. The suspension was stirred for 1 h, and after the volume was adjusted with distilled water. Then, 2 mL of the dilution were transferred to another 100 mL volumetric flask. Distilled water (50 mL) and phenolphthalein (2 drops) were added and neutralized with HCl solution (0.1 N). Iodine solution (2 mL, 2% (w/v)) was added, the volume was adjusted again, and let to rest for 30 min to develop color. The absorbance was recorded at 510 and 620 nm with a spectrophotometer (HP 8453, Hewlett Packard, NY, USA). The amylopectin content was estimated as (100—amylose percentage) [23].

### ζ-Potential

The ζ-potential of AS was determined using a Zetasizer Nano ZS (Malvern Instruments, Ltd, Worcestershire, UK) at room temperature ( $23 \pm 1$  °C). Starch suspensions (0.1%, w/v) were prepared in deionized water at pH 7.0 before analysis [24].

### Total phenolic content

Total phenolic content was measured using the Folin-Ciocalteu method [25, 26]. Briefly, 200 mg of AS were mixed with 2 mL of methanol for 3 h in the absence of light at room temperature ( $23 \pm 1$  °C) [7, 27]. The mixture was centrifuged at  $2740 \times g$  for 10 min at 10 °C and an aliquot of 250 μL was mixed in a test tube with 1250 μL of deionized water and 200 μL of Folin-Ciocalteu reagent. The mixture was allowed to stand for 3 min. After, 300 μL of  $\text{Na}_2\text{CO}_3$  (15%, w/v) were added and the mixture was incubated for 30 min at room temperature ( $23 \pm 1$  °C) in the dark [28]. The absorbance was measured with a spectrophotometer (HP 8453, Hewlett Packard, NY, USA) at 760 nm, and the total phenolic content was expressed as mg of gallic acid equivalents (GAE) per 100 g of starch (db).

### Antioxidant activity by ABTS<sup>•+</sup> assay

The ABTS<sup>•+</sup> assay was employed to determine the antioxidant activity [7]. Previously, the ABTS<sup>•+</sup> radical was prepared from the reaction of 5 mL of 7 mM ABTS with 88 μL of potassium persulfate solution (140 mM). The solution was stored for 16 h at room temperature ( $23 \pm 1$  °C) in the absence of light. After, ethyl alcohol was added to 1 mL of the solution until an absorbance value of  $0.70 \pm 0.05$  at 734 nm was reached. AS samples (200 mg) were mixed with 2 mL of methanol for 3 h in the absence of light at room temperature ( $23 \pm 1$  °C) [7]. The mixture was centrifuged at  $2740 \times g$  for 10 min at 10 °C. An aliquot of 30 μL of the methanolic extract was mixed with 3 μL of ABTS<sup>•+</sup> radical, and after 6 min, the absorbance was taken at 734 nm using a spectrophotometer. The antioxidant activity was expressed as μg of Trolox equivalents (TE)/g of starch (db) employing a Trolox standard curve.

### Antioxidant activity by DPPH<sup>•</sup> assay

For the DPPH<sup>•</sup> assay [29, 30], 200 mg of AS powder and 2 mL of methanol were mixed for 3 h in the absence of light at room temperature ( $23 \pm 1$  °C) [7]. The mixture was centrifuged at  $2740 \times g$  for 10 min at 10 °C. The supernatant (500 μL) was mixed with 2 mL of methanolic DPPH<sup>•</sup> solution (0.06 mmol/L) and incubated for 30 min at room temperature in the dark. The absorbance of the remaining DPPH<sup>•</sup> was measured on a spectrophotometer at 517 nm [31, 32]. The antioxidant activity was expressed as μg of Trolox equivalents (TE)/g of starch employing a Trolox standard curve.

### Scanning electron microscopy (SEM)

The morphology of the AS variations was observed by SEM. A sample of each AS powder was placed directly on the surface of aluminum stubs with carbon adhesive tape and coated with gold for 5 min at 1.5 kV, 5–6 mA in a JFC 1100 vacuum sputter coater (JEOL, Tokyo, Japan). Micrographs were obtained using a scanning electron microscope (JSM-6360, JEOL, Tokyo, Japan) under an accelerating voltage of 13 kV. Magnifications at 250, 1000, and 2000 $\times$  were used [33].

### Particle size distribution

The particle size distribution and Sauter mean diameter ( $D_{3,2}$ ) of the samples were determined on a Mastersizer 3000 laser diffraction particle size analyzer (Malvern Instruments, Malvern, Worcestershire, UK), equipped with a Hydro 2000 module. The samples were analyzed by a wet method, by suspending starch in distilled water, and using refractive

indexes of 1.52 and 1.33, respectively [34]. The polydispersity index (span) and  $D_{3,2}$  values were calculated using Eqs. 1 and 2.

$$D_{3,2} = \frac{\sum_{i=1}^k n_i \cdot D_i^3}{\sum_{i=1}^k n_i \cdot D_i^2} \quad (1)$$

$$\text{span} = (d_{90} - d_{10})/d_{50} \quad (2)$$

where  $D_i$  is the mean diameter of the starch granules;  $n_i$  is the number of starch granules; and  $d_{10}$ ,  $d_{50}$ , and  $d_{90}$  are the diameters at 10, 50, and 90% of cumulative volume, respectively.

### Fourier transform infrared (FTIR) spectroscopy

The spectra of the samples were obtained on an infrared spectrometer (Cary 630, Agilent Technologies, Santa Clara, CA, USA) equipped with an attenuated total reflectance accessory. Dried samples (~0.01 g) were placed in contact with the crystal diamond universal sampling accessory. Measurements were obtained over the range of 4000–400  $\text{cm}^{-1}$  at a resolution of 2  $\text{cm}^{-1}$ . Thirty-two scans per sample were integrated to obtain the mean values of the spectrum [35].

### X-ray diffraction (XRD)

X-ray diffraction patterns of the samples were performed with a diffractometer (Ultima IV X-ray, Rigaku, Tokyo, Japan) [36]. Samples were carried out with filter radiation of Cu-K $\alpha$  ( $\lambda = 1.542 \text{ \AA}$ ), current of 30 mA, a voltage of 40 kV. The samples were analyzed over a  $2\theta$  scan region from 4 to 50° with a step interval of 0.02° (0.5°/min). The relative crystallinity of the samples was calculated using the Jade PRO software (version 7.2, Livermore, CA, USA).

### Gelatinized starch dispersions rheology

AS dispersions (5% w/w) were heated at 90 °C with magnetic stirring for 20 min and left to cool down to 25 °C for 15 min for obtaining gelatinized AS dispersions (GASD) [23]. About 3.8 mL of GASD sample was loaded into the parallel plate geometry (PP50-2, serrated top plate to avoid sample slippage, 50 mm diameter) of a Physica MCR 300 rheometer (Physica Messtechnik GmbH, Stuttgart, Germany). A gap of 0.5 mm between plates was used as some AS granules exhibited sizes of up to about 130  $\mu\text{m}$  (see Results sub-section—“Particle size distribution”), and for allowing for granules swelling upon gelatinization. Samples were allowed to relax for 5 min after loading for structure recovery. Flow curves were determined by varying the shear

rate from 0.01 to 1000  $\text{s}^{-1}$ . The obtained data were described using the following Herschel-Bulkley model:

$$\tau = \tau_0 + K\dot{\gamma}^n \quad (3)$$

where  $\tau$  is shear stress (Pa),  $\tau_0$  is the yield stress (Pa),  $K$  is consistency coefficient ( $\text{Pa s}^n$ ),  $\dot{\gamma}$  is the shear rate ( $\text{s}^{-1}$ ), and  $n$  is the flow behavior index (dimensionless). The viscoelastic properties were determined under oscillatory shear conditions. Initially, the frequency sweeps were carried out in the range 0.01–10 Hz at 0.1% strain for determining the linear viscoelastic region (LVR) of the GASD. Then strain sweeps were carried out in the range from 0.01 to 100% in the LVR range (1 Hz). The storage ( $G'$ ) and loss ( $G''$ ) moduli were obtained with the US200/32 V2.50 software. All the experiments were carried out at 25 °C, and temperature maintenance was achieved with the Physica TEK 150PA Peltier system.

### GASD optical microscopy

GASD were stained with iodine solution (0.1 N) and were observed using an optical microscope (Olympus BX45, Olympus Optical Co., Tokyo, Japan). Micrographs were captured with a digital camera (Olympus C3030, Olympus America Inc., Center Valley, PA, USA). Representative optical micrographs at 40 $\times$  are presented for illustration purposes.

### Swelling power and solubility index

The swelling power (SP) and solubility index (SI) values were determined at 60, 70, 80, and 90 °C, in accordance with Wu et al. [37].

### Water and oil absorption capacities

The water absorption (WAC) and oil absorption (OAC) capacities were determined according to Souza de Castro et al. [17]. The WAC and OAC values were expressed as g of water or oil absorbed per g of starch.

### In vitro digestibility

The in vitro digestion of the raw AS starch purified variations was carried out according to the method of Englyst et al. with slight modifications [38]. Firstly, an enzyme solution was prepared by suspending 1.5 g of pancreatin in 10 mL of 0.02 M sodium acetate buffer (pH 5.5) by magnetic stirring for 30 min. The suspension was centrifuged at 1500 $\times g$  for 10 min, and the supernatant (8 mL) was mixed with 0.4 mL of amyloglucosidase ( $\geq 260 \text{ U/mL}$ ) and 5 mg of invertase [39]. Dried AS starches

(250 mg) were suspended in 20 mL of 0.02 M sodium acetate buffer at pH 5.5. After that, the samples (temperature = 37 °C) were mixed with 5 mL of enzyme solution at 1 min intervals between each sample. Aliquots (0.5 mL) were taken at 20 and 120 min after starting hydrolysis and mixed with 4 mL of absolute ethanol. Then, samples were centrifuged at 3000×g for 5 min, and the glucose content was quantified by glucose oxidase–peroxidase reagent. Starch fractions were classified according to their hydrolysis rate like rapidly digestible starch (RDS), slowly digestible starch (SDS), and resistant starch (RS) using the following equations:

$$\text{RDS (\%)} = \text{G}_{20} \times 0.9 \quad (4)$$

$$\text{SDS (\%)} = (\text{G}_{120} - \text{G}_{20}) \times 0.9 \quad (5)$$

$$\text{RS (\%)} = \text{TS} - (\text{RDS} + \text{SDS}) \quad (6)$$

where TS is the total starch, while G<sub>20</sub> and G<sub>120</sub> are the glucose released at 20 and 120 min, respectively.

## Statistical analysis

All measurements were done by triplicate, and data were presented as the means ± standard deviation. Data were processed using one-way analysis of variance (ANOVA) and Tukey's means comparison analysis with a significance level of  $p < 0.05$ . Pearson's correlation coefficients were calculated to identify trends between total phenolic content and antioxidant activity. Data analysis was carried

out using the SPSS software (version 26.0.0.0, Chicago, IL, USA).

## Results and discussion

### Yield and chemical composition

Table 1 presents the results of the proximal chemical composition of the AS variations. AS<sub>F0P0</sub> presented the highest carbohydrate content (85.15 ± 0.04%), which could be attributed to the reduction of lipids and proteins [7]. However, this sample presented the lowest extraction yield (16.15 ± 1.62%). The lipid content was significantly diminished by defatting treatment in AS<sub>F0</sub> and AS<sub>F0P0</sub> starches. The lipid content of all AS was lower (0.15–1.02%) than that reported (3.4–6.9%) by García-Silveira et al. [7]. Starch lipids can be classified as internal and external, but their removal efficiency may be related to the solvent used and plant source [40, 41]. In general, petroleum ether (non-polar solvent) is usually used to extract free lipids and other non-polar compounds from cereals flour [40, 42]. Similarly, AS<sub>P0</sub> and AS<sub>F0P0</sub> starches presented lower protein content than AS<sub>L</sub> and AS<sub>F0</sub>. Protein contents of 14.7–17.4% have been reported for annatto starches extracted by water, acid, and alkaline methods [7]. Decreased protein content in alkali-treated starches has been associated with the solubilization of inner and surface starch granule proteins [11, 43]. Besides, the amylose and amylopectin contents were modified by the applied purification treatments. The low percentage of amylose in AS<sub>L</sub> could be due to an underestimation caused by the high lipid content, while the amylose content of defatted AS<sub>F0</sub> was significantly higher than for

**Table 1** Proximal chemical composition, yield, and ζ-potential of annatto starches (AS) variations

	Annatto starch			
	AS <sub>L</sub>	AS <sub>F0</sub>	AS <sub>P0</sub>	AS <sub>F0P0</sub>
Moisture* (%)	8.63 ± 0.01 <sup>c</sup>	9.83 ± 0.16 <sup>b</sup>	11.45 ± 0.13 <sup>a</sup>	11.26 ± 0.01 <sup>a</sup>
Ash (%)	2.49 ± 0.01 <sup>a</sup>	2.35 ± 0.03 <sup>a</sup>	2.55 ± 0.08 <sup>a</sup>	2.08 ± 0.05 <sup>b</sup>
Lipid (%)	1.02 ± 0.04 <sup>a</sup>	0.28 ± 0.04 <sup>b</sup>	1.01 ± 0.01 <sup>a</sup>	0.15 ± 0.06 <sup>b</sup>
Protein (%)	7.51 ± 0.07 <sup>a</sup>	7.52 ± 0.36 <sup>a</sup>	5.81 ± 0.01 <sup>b</sup>	4.36 ± 0.03 <sup>c</sup>
Fiber (%)	7.09 ± 0.67 <sup>b</sup>	6.49 ± 0.74 <sup>b</sup>	9.21 ± 0.19 <sup>a</sup>	8.25 ± 0.04 <sup>ab</sup>
Carbohydrates (%)	81.9 ± 0.63 <sup>bc</sup>	83.37 ± 0.37 <sup>b</sup>	81.43 ± 0.11 <sup>c</sup>	85.15 ± 0.04 <sup>a</sup>
Apparent amylose (%)	20.76 ± 0.66 <sup>c</sup>	28.56 ± 0.89 <sup>a</sup>	25.16 ± 0.86 <sup>b</sup>	18.94 ± 1.04 <sup>d</sup>
Amylopectin (%)	79.24 ± 0.67 <sup>b</sup>	71.44 ± 0.89 <sup>d</sup>	74.84 ± 0.86 <sup>c</sup>	81.06 ± 1.04 <sup>a</sup>
Yield (%)	22.55 ± 1.68 <sup>a</sup>	20.05 ± 0.52 <sup>ab</sup>	17.46 ± 0.96 <sup>bc</sup>	16.15 ± 1.62 <sup>d</sup>
ζ-Potential	− 23.80 ± 0.99 <sup>a</sup>	− 20.30 ± 0.42 <sup>b</sup>	− 18.30 ± 0.01 <sup>b</sup>	− 24.10 ± 0.85 <sup>a</sup>

Data are means ± standard deviations. Different letters in the same row indicate a significant difference between treatments ( $p < 0.05$ ). AS<sub>L</sub> (low purity); AS<sub>F0</sub>: starch from defatted flour (medium purity); AS<sub>P0</sub>: starch from deproteinized flour (medium purity); AS<sub>F0P0</sub>: starch from defatted and deproteinized flour (high purity)

\*Moisture expressed on a wet basis

non-defatted AS<sub>L</sub> and AS<sub>P0</sub>, may be due to a breakdown of the amylose–lipid complexes [40]. In contrast, protein removal decreased the amylose content, especially in AS<sub>F0P0</sub>, probably by an amylose leaching caused by the alkaline solution [44]. In general, starches can be classified as low (or waxy) (8–22%), intermediate (23–27%), or high amylose content (28–32%). Considering this type of classification, AS variations are of intermediate amylose content. Within this category, other starches from various plant sources have been reported, such as some varieties of wheat, potato, corn, and rice [45–47].

## ζ-Potential

The ζ-potential values of the AS variations are shown in Table 1. This parameter is helpful to study the electric interactions of components in foods. The ζ-potential reflects the potential between the liquid layer immediately next to the surface (firmly bound to the particle) and the continuous phase [48]. All the AS variations were negatively charged, with values ranging from – 18.30 to – 24.10 mV. Similar values of ζ-potential have been reported for taro starch granules (– 20.3 ± 0.3 mV), melloco seed starch (about – 24 mV), and Ibes bean starch (– 26.26 ± 2.30 mV) [23, 24, 49]. In emulsions, it is reported that a ζ-potential between – 11 and – 20 mV is not enough to prevent particle agglomerations induced by Van der Waals forces. Values greater than – 30 mV are needed to produce suitable electrostatic repulsions and thus ensure the stability of the dispersed particles [24, 50]. In general, it is assumed that the negative ζ-potential value of starch is due to the carboxyl groups present on their surface, and the presence of lipids and proteins could modify the ζ-potential value [51]. The removal of lipids from AS caused a significant decrease in ζ-potential. The lipid composition of annatto seeds is made up of palmitic, linoleic, and oleic acids [52]. These fatty acids are hydrophobic molecules that can contribute with negative carboxyl groups (–COO<sup>–</sup>) to annatto starch granules in their free form [51]. The lipid removal could cause a reduction in the negative charges, inducing a significant diminution in the ζ-potential value of AS<sub>F0</sub> (Table 1). On the other hand,

annatto seed residues are characterized by the presence of aromatic, non-polar and basic amino acids as phenylalanine + tyrosine, leucine, and lysine, respectively [5]. Lysine has an amine group (–NH<sub>3</sub><sup>+</sup>) in its side chain with a positive charge at pH 7.0 that could influence the ζ-potential of annatto starch. The deproteinization of AS<sub>F0P0</sub> could have induced an increase in the net negative charge of starch due to a reduction of the positive charges. Wongsagnon et al. [53] reported that the ζ-potential of rice flour changed depending on the pH and the protein content, although the exchange rate was variable. Under acidic conditions (pH 2), the ζ-potential became more positive at higher protein contents, while in an alkaline medium (pH 12), ζ-values were more negative with increasing protein percentage. On the other hand, at pH 7, there was a non-significant difference in ζ-potential. Some other factors, such as phosphate groups and amylose content, have been reported to modify the ζ-potential of starches [53, 54]. Bixin and norbixin carotenoids could influence the ζ-potential of annatto starches, and this is a topic worth investigating in the future.

## Total phenolic content and antioxidant activity

Table 2 presents the total phenolic content (TPC) and antioxidant activity of the AS variations by ABTS<sup>•+</sup> and DPPH<sup>•</sup> assays. The TPC varied from 6.70 ± 0.23 mg of GAE/100 g for AS<sub>L</sub> (lowest purity) to 3.16 ± 0.44 mg of GAE/100 g for AS<sub>F0P0</sub> (highest purity). Unpurified isolated starches from annatto seed residues have been reported to have phenolic compounds contents of 1306–1454 mg of GAE/100 g, which may be due to their higher protein and fiber content [7]. Other starches isolated from unconventional sources present quite variable TPC, including 8.2 ± 0.1 mg of GAE/100 g for babassu starch and 6062.6 ± 14 mg of GAE/100 g for pitomba endocarp starch [17, 29]. Hypolaetin (pentahydroxyflavone) is the main phenolic compound reported in annatto seeds, followed by the caffeoyl acid derivative [55]. Generally, phenolic acids and flavonoids are present as soluble conjugates (glycosides) and insoluble forms covalently linked to components such as structural proteins [56]. Also, phenolic compounds interact with starch through

**Table 2** Total phenolic content and antioxidant activity of annatto starch (AS) variations

	Total phenolic content (mg of GAE/100 g of starch)	ABTS <sup>•+</sup> assay (μg of TE/g of starch)	DPPH <sup>•</sup> assay (μg of TE/g of starch)
AS <sub>L</sub>	6.70 ± 0.23 <sup>a</sup>	1.14 ± 0.13 <sup>a</sup>	0.47 ± 0.03 <sup>a</sup>
AS <sub>F0</sub>	6.71 ± 0.63 <sup>a</sup>	1.07 ± 0.08 <sup>a</sup>	0.36 ± 0.01 <sup>b</sup>
AS <sub>P0</sub>	5.54 ± 0.22 <sup>b</sup>	0.52 ± 0.09 <sup>b</sup>	0.35 ± 0.02 <sup>b</sup>
AS <sub>F0P0</sub>	3.16 ± 0.44 <sup>c</sup>	0.62 ± 0.04 <sup>b</sup>	0.09 ± 0.01 <sup>c</sup>

Data are means ± standard deviations. Different letters in the same column indicate a significant difference between treatments ( $p < 0.05$ ). AS<sub>L</sub> (low purity); AS<sub>F0</sub>: starch from defatted flour (medium purity); AS<sub>P0</sub>: starch from deproteinized flour (medium purity); AS<sub>F0P0</sub>: starch from defatted and deproteinized flour (high purity)

non-covalent bonds, such as hydrogen bonds, hydrophilic interactions, and ionic and electrostatic interactions [57]. Statistical analysis showed that TPC in annatto starches decreased when soluble proteins were removed. This decrease could be due to the alkaline deproteinization treatment since the ester bonds that bind phenolic compounds with proteins and carbohydrates are broken [56].

The antioxidant activity also decreased significantly in AS subjected to alkaline treatment to remove proteins. In the antioxidant activity assay by the ABTS<sup>•+</sup> radical, AS<sub>L</sub> and AS<sub>F0</sub> starches presented the highest radical scavenging activity (Table 2). These results were lower than those reported for unpurified annatto starchy materials (1.9–3.6 mg of TE/g of the sample), which also had a high content of phenolic compounds and carotenoids [7]. Again, the process of removing soluble proteins led to a significantly decreased scavenging activity in AS<sub>P0</sub> and AS<sub>F0P0</sub> starches. The antioxidant activity assay by DPPH<sup>•</sup> radical also showed a significant decrease in antioxidant activity of the AS variations, with values ranging from  $0.47 \pm 0.03$  to  $0.09 \pm 0.01$  µg of TE/g of starch. Therefore, AS<sub>L</sub> was the treatment that presented the highest donor capacity of hydrogen atoms or electrons to reduce the DPPH<sup>•</sup> radical [3]. In the present study, there is a positive correlation between the content of phenolic compounds and the antioxidant activity by ABTS<sup>•+</sup> ( $r = 0.667$ ,  $p < 0.01$ ) and DPPH<sup>•</sup> ( $r = 0.898$ ,  $p < 0.01$ ) assays (see Supplementary Material—Table S1), suggesting that the antioxidant activity of AS variations was influenced by the content of total phenolic compounds, which agrees with the literature [28, 58].

### Morphology of starch granules

SEM micrographs of the AS variations are shown in Fig. 1. In all cases, the granules presented a heterogeneous morphology characterized by an array of oval (predominant), spherical, triangular, and irregular shapes. These morphologies agree with those reported previously for annatto starch granules [6–8]. The AS<sub>L</sub> granules surface was mostly smooth, with rounded edges, without pores, cracks, or holes (Fig. 1A). However, the purified variations tended to show increasingly irregular shapes, defects (pores, cracks, and holes), and debris vestiges (Fig. 1B–D). In particular, the surging of these irregularities was intensified in the deproteinization treatment (AS<sub>P0</sub>; Fig. 1C) and the combined defatting-deproteinization treatment (AS<sub>F0P0</sub>; Fig. 1D3). The irregular shapes increase could be due to granule coalescence into single structures, as has been reported by alkaline treatment of pea [11] and wheat [43] starches that induced a partial gelatinization and adhesion of starch granules. Debris formation can be attributed to AS granules disintegration due to purification treatment [59]. In all treatments, non-starchy materials were present, such as membrane debris,

elongated woody-looking forms, irregular spongy bodies, and parenchyma remains. The starch granules could adhere to these impurities and form agglomerates that changed slightly in abundance according to the AS purity degree. AS<sub>L</sub> presented the highest agglomerates, while the number of agglomerates decreased in AS<sub>F0</sub>, AS<sub>P0</sub>, and AS<sub>F0P0</sub>. Therefore, the defatting and protein elimination processes could have eliminated part of the remaining lipids and proteins that favored the agglomeration of the starch granules to non-starchy materials.

### Particle size distribution

Table 3 shows that  $D_{3,2}$  increased when soluble proteins were removed from the AS. A similar trend was found for wheat starch treated with 0.25% NaOH, which showed a significant increase in the average granule, attributed to a partial gelatinization of the starch granules [43]. The AS variations showed a bimodal particle size distribution pattern with a central peak between 118.8 and 134.9 µm and a smaller peak between 22.6 and 25.7 µm (Fig. 1). Zabot et al. [8] reported a bimodal particle size distribution pattern for AS with the central peak near 10 µm and a smaller peak near 100 µm, while García-Silveira et al. [7] reported a polymodal distribution in AS extracted with an alkaline process. The disagreements in the distribution pattern reported by these authors and by us could be due to the intensity of the treatments used in each case. In our case, the purification treatments, while being capable of depleting the lipid/protein content, did not cause extensive disintegration of the AS granules. Starch granules modification by the alkaline deproteinization was such that it promoted the granules coalescence, leading to increased particle sizes. These results are backed up by the cumulative volumes  $d_{10}$ ,  $d_{50}$ , and  $d_{90}$  and the rather high span (2.57–2.77) values (Table 3), which tended to increase significantly in the following relative order: AS<sub>L</sub> < AS<sub>F0</sub> < AS<sub>P0</sub> < AS<sub>F0P0</sub>.

### FTIR spectroscopy

FTIR spectra (Fig. 2a) revealed the short-range order of the AS variations. The absorption peaks showed a similar structure to those from non-conventional native starches, such as inhambu and cassava starches [60, 61]. Regardless of the degree of purification of the AS, the four studied samples had remarkably similar IR spectra and intensity. All FTIR spectra exhibited a broader peak at  $3273 \text{ cm}^{-1}$ , which can be associated with the O–H bond stretching of amylose and amylopectin chains [62]. The peak near  $2100 \text{ cm}^{-1}$  can be attributed to free water content, suggesting that water molecules play a structural role in the starch [63]. A band at  $1635 \text{ cm}^{-1}$  can be assigned to amide-I stretching vibrations, and the doublet peak at

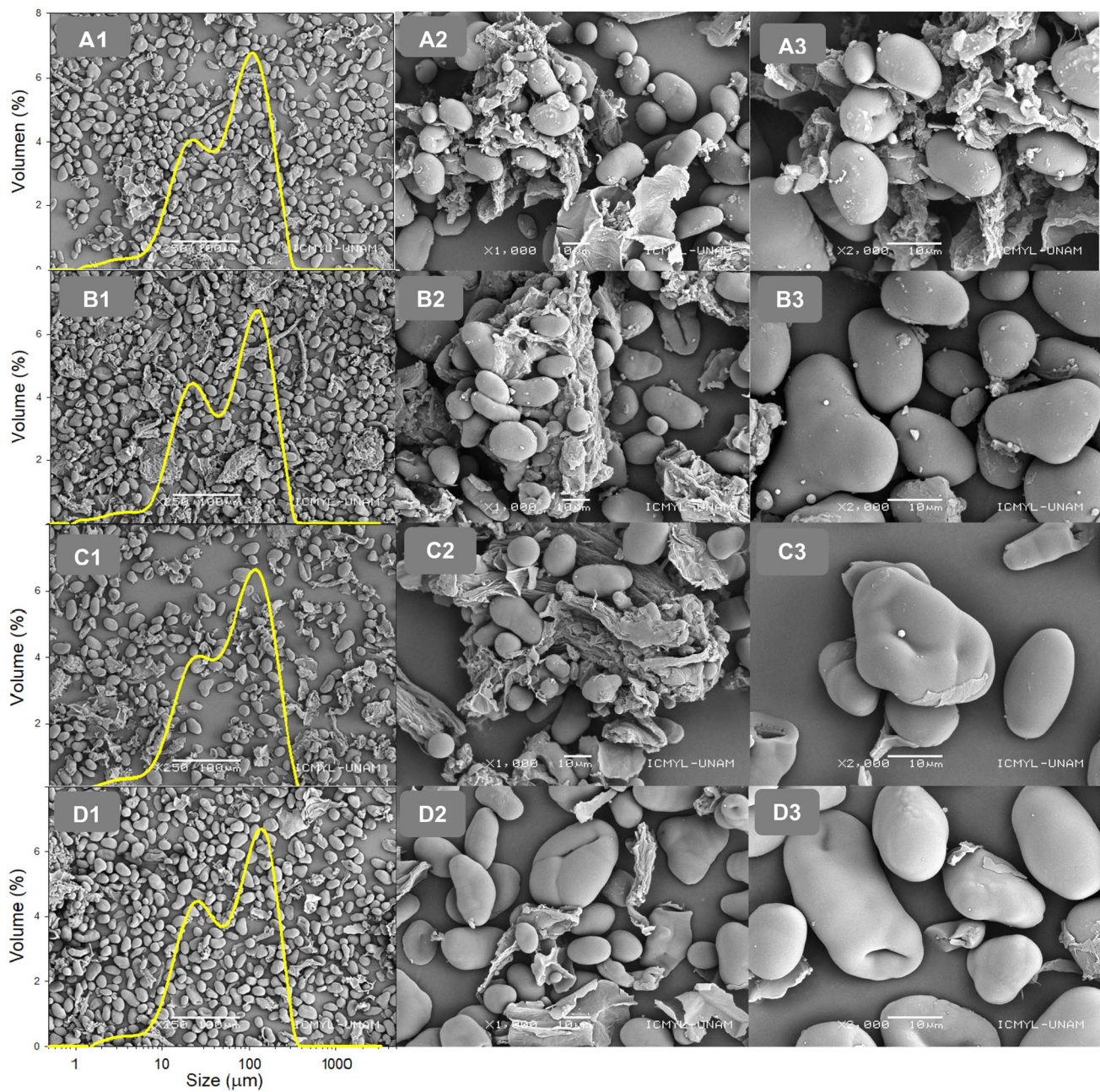


**Fig. 1** SEM micrographs and particle size distribution of annatto starch (AS) variations: **A**  $AS_L$  (low purity); **B**  $AS_{F0}$ ; starch from defatted flour (medium purity); **C**  $AS_{P0}$ ; starch from deproteinized

flour (medium purity); **D**  $AS_{F0P0}$ ; starch from defatted and deproteinized flour (high purity). Magnifications: (1) 250 $\times$ , (2) 1000 $\times$ , (3) 2000 $\times$

**Table 3** Sauter mean diameter ( $D_{3,2}$ ) and the granule diameters at 10% ( $d_{10}$ ), 50% ( $d_{50}$ ), and 90% ( $d_{90}$ ) cumulative volumes, of annatto starch (AS) variations

	$d_{10}$ ( $\mu\text{m}$ )	$d_{50}$ ( $\mu\text{m}$ )	$d_{90}$ ( $\mu\text{m}$ )	$D_{3,2}$ ( $\mu\text{m}$ )	Span
$AS_L$	$13.07 \pm 0.18^c$	$63.33 \pm 1.31^{ab}$	$178.07 \pm 1.83^d$	$26.80 \pm 0.48^b$	$2.57 \pm 0.17^b$
$AS_{F0}$	$13.20 \pm 0.39^c$	$63.05 \pm 4.87^b$	$183.23 \pm 3.90^c$	$26.35 \pm 1.18^b$	$2.71 \pm 0.16^{ab}$
$AS_{P0}$	$14.30 \pm 0.17^b$	$65.73 \pm 1.38^{ab}$	$190.70 \pm 6.75^b$	$30.43 \pm 0.31^a$	$2.69 \pm 0.15^{ab}$
$AS_{F0P0}$	$14.57 \pm 0.14^a$	$66.21 \pm 1.99^a$	$197.93 \pm 5.92^a$	$31.09 \pm 0.38^a$	$2.77 \pm 0.16^a$

Data are means  $\pm$  standard deviations. Different letters in the same column indicate a significant difference between treatments ( $p < 0.05$ ).  $AS_L$  (low purity);  $AS_{F0}$ ; starch from defatted flour (medium purity);  $AS_{P0}$ ; starch from deproteinized flour (medium purity);  $AS_{F0P0}$ ; starch from defatted and deproteinized flour (high purity)



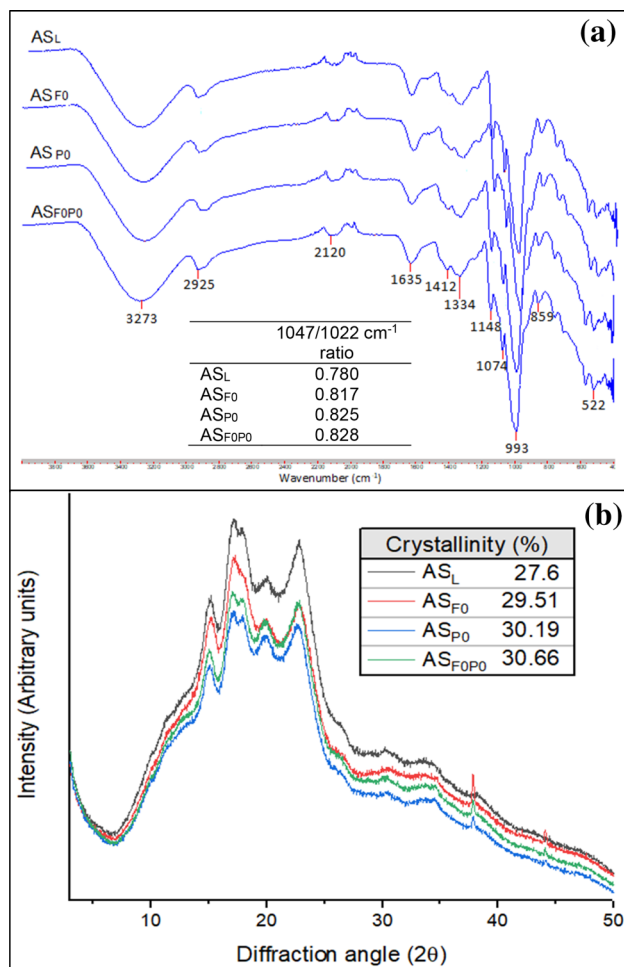


**Fig. 2** **a** FTIR spectra and **b** XRD patterns of annatto starch (AS) variations. AS<sub>L</sub> (low purity); AS<sub>F0</sub>: starch from defatted flour (medium purity); AS<sub>P0</sub>: starch from deproteinized flour (medium purity); AS<sub>F0P0</sub>: starch from defatted and deproteinized flour (high purity)

1412–1334  $\text{cm}^{-1}$  can be attributed to the inflection of N–H bonds and the stretching of C–N bonds [62, 64]. Therefore, these peaks corroborate the presence of protein molecules, even in the AS variations that underwent deproteinization treatment. Other signals were present at 2925  $\text{cm}^{-1}$  and 1412  $\text{cm}^{-1}$ , which could be attributed due to the asymmetrical stretching and angular deformation of the C–H bond of the glucose ring [63]. The fingerprint region stood out two peaks at 1148  $\text{cm}^{-1}$  and 1074  $\text{cm}^{-1}$  corresponding to the C–C and C–O–H flections of the glycosidic bond of starch, while the intense peak at 993  $\text{cm}^{-1}$  corresponds to the crystalline region of the starch [12, 43, 62]. The remarkable similarity in peaks and signal intensity between the treatments suggests that lipid and protein removal did not modify the chemical structure of AS. The 1047/1022  $\text{cm}^{-1}$  intensity ratio was used to estimate the ratio of amorphous to crystalline domains (Fig. 2a) [23]. The bands at 1047  $\text{cm}^{-1}$  and 1022  $\text{cm}^{-1}$  are

associated with crystalline and amorphous fractions [12]. The 1047/1022  $\text{cm}^{-1}$  intensity ratio of the AS increased when the soluble proteins were removed, suggesting a slight increase in the proportion of the ordered forms.

## XRD analysis

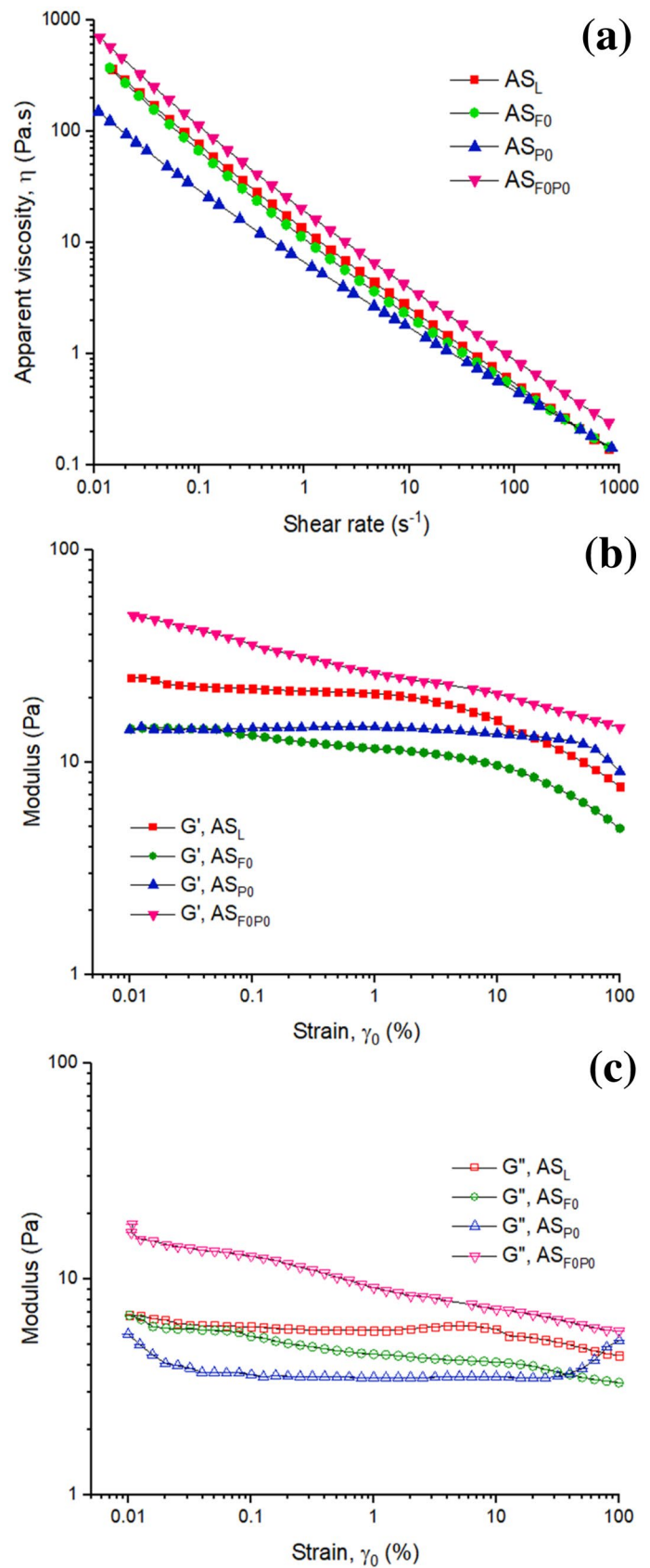
The semicrystalline structure of starch granules presents a characteristic diffraction pattern that allows its identification. Starches can be classified as A-type (generally present in cereals), B-type (from tubers), C-type (from some seeds and leguminous), and V-type (starches in complex with other agents like fatty acids and emulsifiers) [65]. The AS diffractograms (Fig. 2b) presented high-intensity peaks at approximately 15.1, 17–18, 19.9, and 22.7°  $2\theta$ . This pattern corresponds to the typical A-type crystalline structure [66] and agrees with the diffraction pattern reported by Zabot et al. [8] for annatto starch. The A-type starches are characterized by a compact structure presenting a central double helix inside the unit cell of double helices [65, 66]. Garcia-Silveira et al. [7] reported a C-type (presenting both A- and B-type signals) for annatto starch. Nevertheless, the peak associated with B-type polymorphism (6°  $2\theta$ ) was absent in this work. The defatting and alkaline deproteinization did not modify the diffraction patterns of AS, while the morphology and amylose contents were different. Wang and Copeland [44] reported amylose leaching in pea starches after soaking in 0.1 M NaOH solution. They attributed a modification of the internal structure that was physically observed as a depression in the center of the starch granule. In the same way, the alkaline deproteinization altered the structure of the granules. When starch granules undergo amylose leaching, the internal structure is modified, and a physical depression can be observed in the AS<sub>F0P0</sub> granules (Fig. 1D3). Also, the AS samples showed a slight increase in their semicrystalline percentage (Fig. 2b) when the native proteins were eliminated. This increase was consistent with the increase in the intensity ratio of 1047/1022  $\text{cm}^{-1}$  obtained in the FTIR analysis, indicating a more orderly structure.

## Rheological measurements

All the gelatinized AS dispersion variations presented a non-Newtonian behavior, characterized by shear-thinning under the applied shear rate (Fig. 3a). A shear-thinning behavior is associated with an alignment of the biopolymer molecules with the field of shear changing its original conformation; also, biopolymer-biopolymer interactions are disrupted, reducing the force between the stream layers [10, 15]. The steady flow profiles were well described ( $R^2 > 0.98$ ) by the Herschel-Bulkley model.

All the GASD required of the application of shear stress that exceeded the yield stress ( $\tau_0$ ) of the gelatinized

**Fig. 3** Rheological properties of gelatinized AS dispersions (5% w/w) at 25 °C: **a** Flow curves; **b** Storage ( $G'$ ) and **c** loss ( $G''$ ) moduli depending on strain (%) obtained from oscillatory tests at 1 Hz.  $AS_L$  (low purity);  $AS_{F0}$ : starch from defatted flour (medium purity);  $AS_{P0}$ : starch from deproteinized flour (medium purity);  $AS_{F0P0}$ : starch from defatted and deproteinized flour (high purity)



dispersions for flow to commence, which was from higher to lower:  $AS_{F0P0}$  ( $5.51 \pm 1.23$  Pa) >  $AS_L$  ( $4.08 \pm 0.92$  Pa) >  $AS_{F0}$  ( $3.25 \pm 1.43$  Pa) >  $AS_{P0}$  ( $0.92 \pm 0.36$  Pa).  $\tau_0$  may be considered as a threshold critical value for the gelatinized dispersions to begin to deform. The same order was presented by  $K$  values varying as follows:  $AS_{F0P0}$  ( $13.71 \pm 0.99$ ) >  $AS_L$  ( $9.83 \pm 1.20$ ) >  $AS_{F0}$  ( $6.70 \pm 0.67$ ) >  $AS_{P0}$  ( $5.74 \pm 0.24$ ). The flow index varied from higher to lower values as follows:  $AS_{P0}$  ( $0.45 \pm 0.01$ ) >  $AS_{F0}$  ( $0.42 \pm 0.02$ ) >  $AS_{F0P0}$  ( $0.39 \pm 0.01$ ) >  $AS_L$  ( $0.36 \pm 0.02$ ). The decrease in  $K$  values showed a lower resistance of AS gels to flow, while lower  $n$  values refer to a more pronounced pseudoplastic behavior ( $n < 1$ ). The apparent viscosity ( $\eta$ ) exhibited by the GASD as a function of  $\dot{\gamma}$ , was calculated with the following expression:  $\eta = \tau_0 + K\dot{\gamma}^{n-1}$ . The apparent viscosity at any shear rate value was higher for  $AS_{F0P0}$  followed by  $AS_L > AS_{F0} > AS_{P0}$  variations. The differences in  $\eta$  could be associated with the purity degree of the GASD variations. When starch granules are gelatinized in water excess, they reach their maximum swelling degree and begin to break down, releasing amylose and amylopectin molecules. However, structural granular residues, called “ghosts”, also remain, which can also be associated with endogenous proteins and lipids [67, 68]. Therefore, the content of proteins and lipids greatly influences the rheological behavior of gelatinized starches. The present results suggest that lipids and proteins provided rigidity to the gelatinized starch, increasing the viscosity of the  $AS_L$  matrix. Defatting and deproteinization induced a reduction in the flow resistance of  $AS_{F0}$  and  $AS_{P0}$ , which may be due to a breakdown of the protein-starch and lipid-starch bonds, resulting in a more fragile structure [10]. However, the viscosity of the gel increased when starch was purified by combining defatting with deproteinization ( $AS_{F0P0}$ ). This behavior can be explained by light microscopy observations (see Supplementary Material—Fig. S2). The micrographs showed whole and more defined gelatinized granules in starch gels with higher lipid and protein content ( $AS_L$ ,  $AS_{F0}$ , and  $AS_{P0}$ ), in addition to presenting a more widely spaced distribution. In  $AS_{F0P0}$ , the optical micrographs showed the presence of broken, irregular, and leached starch granules, forming a more compact and homogeneous gel structure. This observation is consistent with the SEM micrographs (Fig. 1), where increasing granule damage was associated with intense starch purification.

Regarding the viscoelastic properties of GASD, Fig. 3b shows the storage modulus ( $G'$ ), and Fig. 3c shows the loss modulus ( $G''$ ) as a function of the strain. For all the GASD variations,  $G'$  was higher than  $G''$ , indicating a predominant solid-like behavior. A similar behavior was observed for bean starch gels at a 5% (w/w) [23]. At percentages of strain less than 10%, both the  $G'$  and  $G''$  moduli remained practically constant, indicating a nearly Newtonian behavior. In the linear viscoelastic zone (0.1% of strain), the  $G'$

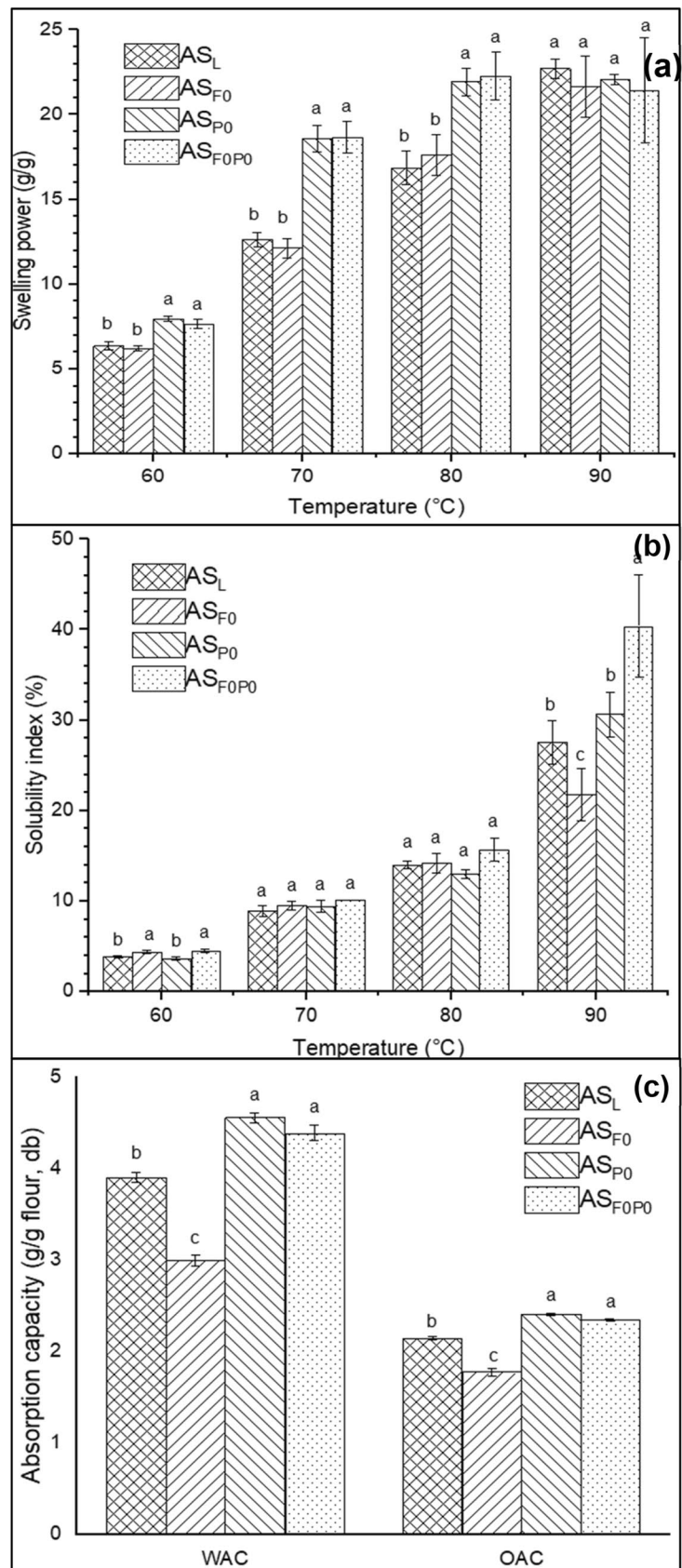
value of  $AS_{F0P0}$  gel (35.87 Pa) was higher than for the  $AS_L$ ,  $AS_{P0}$ , and  $AS_{F0}$  gels (22.07, 14.49, and 13.15 Pa, respectively) (Fig. 3b). The solid-like behavior of  $AS_{F0P0}$  gel was  $\sim 1.62$ ,  $\sim 2.47$ , and  $\sim 2.72$  times higher than  $AS_L$ ,  $AS_{P0}$ , and  $AS_{F0}$  gels, respectively. This trend was similar at 10% of strain, where  $AS_{F0P0}$  (21.01 Pa) presented a higher value in  $G'$  than  $AS_L$ ,  $AS_{P0}$ , and  $AS_{F0}$  gels (15.79, 13.62, and 9.68 Pa, respectively). At 100% strain, the  $G'$  values followed the order of  $AS_{F0P0}$  (14.60 Pa) >  $AS_{P0}$  (9.06 Pa) >  $AS_L$  (7.69 Pa) >  $AS_{F0}$  (4.89 Pa). The drop in the  $G'$  modulus corresponds to a breakdown of the three-dimensional gel structure with an alignment of the polymeric chains in the direction of the flow field [69]. When comparing the response of each of the treatments to the oscillatory stress test, it is observed that endogenous lipids and proteins play a role in the strength of the starch hydrogel. At low strain percentages,  $AS_L$  presented higher values in modulus  $G'$  than  $AS_{F0}$  and  $AS_{P0}$ , corroborating that the presence of proteins increased the storage modulus of gelatinized starch [70]. Still,  $AS_{F0P0}$  presented higher  $G'$  values than the other treatments, according to the steady shear results (Fig. 3a). These results support the proposal that both lipids and proteins provide some structural rigidity to the gel, mainly at low percentages of strain (< 10%). At the same time, starch purification (defatting plus deproteinization) increases the granule fragility leading to a release of polymeric compounds during gelatinization and therefore enhancing the solid-like behavior of the AS gel.

## Functional properties

The swelling power (SP) and solubility index (SI) values provide information about the degree of interaction between the chains present in the crystalline and amorphous regions of the starch granule [71]. Figure 4a shows that the SP depended on the purity degree of AS. Other authors have reported an enhanced SP in rice flours submitted to a protein removal [9]. As expected, AS submitted to deproteinization treatment presented a higher SP due to ionization of the hydroxyl groups that negatively charge the starch molecules [13]. The change in the charges induces a repulsion inside the structure, increasing the water filtration and augmenting the swelling volume [13]. The maximum SP was presented at 90 °C in the different AS (21.44–22.71 g water/g starch). Our studied starches presented similar SP to that reported for some Indian wheat varieties (20.2–24.9 g/g) [71]. When starch granules are heated in water, water molecules associate with amylose and amylopectin fractions by hydrogen bonds developed within the hydroxyl groups [13]. Therefore, to a higher degree of water association, starch swelling was increased.

As in the SP, the SI increased throughout the entire temperature range independently of the purity degree, from

**Fig. 4** **a** Swelling power, **b** solubility index, and **c** water and oil absorption capacities (WAC and OAC) of annatto starch (AS) variations. Different letters on the same group mean significant differences ( $p < 0.05$ ). AS<sub>L</sub> (low purity); AS<sub>F0</sub>: starch from defatted flour (medium purity); AS<sub>P0</sub>: starch from deproteinized flour (medium purity); AS<sub>F0P0</sub>: starch from defatted and deproteinized flour (high purity)



3.67% to 40.43% (Fig. 4b). It has been reported that wheat and maize starches have solubilities of 20% and 18%, respectively, at 95 °C [72]. At the beginning of the heating, the granule structure begins to lose, and the amylose fraction starts to leach and dissolve in the aqueous medium with the rise of temperature [68]. The main difference in the SI was observed at 90 °C, where  $AS_{F0P0}$  reached the highest solubility (Fig. 4b). When the surface proteins of the starch granules are present, the swelling and the solubility are restricted; however, by increasing the starch purity, these functional properties are enhanced due to an augmented exposure of the granule to water molecules [41]. On the other hand, the amylose chains restrict the swelling; therefore, the amylose leaching from the amorphous fraction favored the SP and SI [13].

The water absorption (WAC) ranged between 3.9 and 4.6 g water/g starch and the oil absorption (OAC) between 1.8 and 2.4 g oil/g starch (Fig. 4c). Our results are similar to the WAC reported for defatted macadamia flours (4.71–6.72 g water/g flour, db) and superior to the OAC of corn and rice starches (0.80–1.1 g oil/g starch, db) [73, 74]. The hydrophilic tendency of the starch strongly depends on the open spaces for water penetration and the available water binding sites in the starch granule [41]. In our study,  $AS_{P0}$  and  $AS_{F0P0}$  presented the greatest WAC and OAC values, which could be associated with their fiber content (Table 1). It is reported that fiber content increases the hydration properties due to the hydroxyl group interaction between fiber and water molecules through hydrogen bonds [58]. According to the high values of WAC and OAC, AS could be used as an additive in food products that require high retention of oil or water [17].

### In vitro digestibility

The in vitro digestibility of the raw AS variations is shown in Fig. 5. All samples presented a higher fraction of slowly digestible starch (SDS) than rapidly digestible starch (RDS) and resistant starch (RS). RDS and SDS percentages were similar to the content reported in high amylose rice starch (20.8% of RDS and 40.7% of SDS) [75]. The SDS percentage increased significantly with respect to the RDS and RS fractions when AS was defatted ( $AS_{F0}$ ), deproteinized ( $AS_{P0}$ ), or defatted/deproteinized ( $AS_{F0P0}$ ), but these increases were non-significantly different. The RDS starch fraction also increased significantly as the AS starch was defatted, deproteinized or defatted/deproteinized, and exhibited significant differences between treatments, as follows in increasing order:  $AS_L < AS_{F0} < AS_{P0} < AS_{F0P0}$ . Our results are in agreement with studies of the in vitro digestion of rice starch subjected to defatting and deproteinization [9]. These results can be attributed to the enzyme access to restricted substrate sites as lipid and protein removal, which allowed

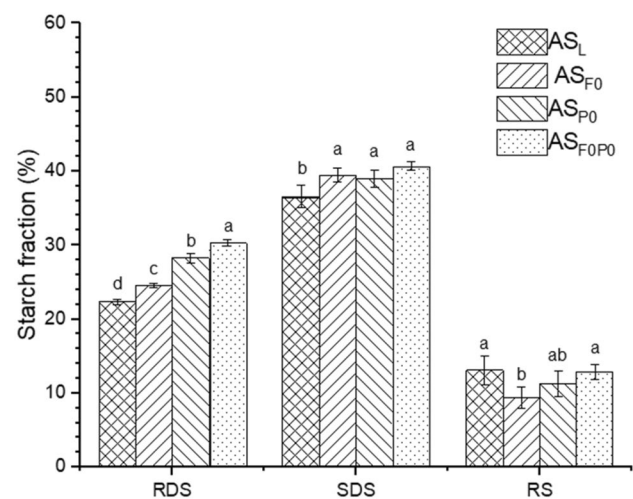


**Fig. 5** Annatto starch (AS) digestibility assay as a function of starch purity. Different letters on the same group mean significant differences ( $p < 0.05$ ).  $AS_L$  (low purity);  $AS_{F0}$ : starch from defatted flour (medium purity);  $AS_{P0}$ : starch from deproteinized flour (medium purity);  $AS_{F0P0}$ : starch from defatted and deproteinized flour (high purity). RDS rapidly digestible starch; SDS slowly digestible starch; RS resistant starch

an easier migration of pancreatic  $\alpha$ -amylase into the starch granule. Thus, the susceptibility to hydrolysis by digestive enzymes of amylose and amylopectin increased [75]. Previous reports of alkali-treated pea starch showed an increased in vitro enzymatic breakdown when protein content was diminished [44]. As mentioned before, the chemical composition, SEM, and XRD results suggest that the deproteinization treatment can cause an amylose leaching of the AS granules. Consequently, the amylose chains breaking, and the augmented amylopectin fraction could facilitate the enzymatic attack. The short branched chains of amylopectin are weak points in the crystalline structure, resulting in augmented hydrolysis susceptibility, increasing RDS percentage [10, 76]. Resistant starch contents remained relatively unchanged for treatments including deproteinization ( $AS_{P0}$  and  $AS_{F0P0}$ ) but decreased significantly for  $AS_{F0}$  concerning to RS content of  $AS_L$ .

### Conclusion

Annatto flour was obtained from depigmented annatto seeds, and was purified via soaking in sodium metabisulfite solution, defatting, deproteinization and combined defatting/deproteinization. The removal of protein decreased phenolic compounds and antioxidant activity of AS, while the depletion of lipids and proteins did not change the basic chemical structure of AS. However, the functional properties (swelling power, solubility index, water and oil absorption), and the flow and oscillatory viscoelastic properties of

gelatinized starch dispersions were significantly higher as the AS purity degree was increased. Independently of the purification degree of AS, the slowly digestible starch fraction predominated over that of the readily digestible starch and resistant starch fractions. Overall, the results showed that annatto seeds are viable sources of starch with marked antioxidant capacity, while exhibiting acceptable gel rheological properties. These results pinpoint the feasibility of using annatto starch as an alternative starch source in food applications requiring high water and oil retention capabilities, and where relative low starch digestibility is desired. Also, AS can be incorporated in the preparation of bread to improve antioxidant properties and textural characteristics.

**Supplementary Information** The online version contains supplementary material available at <https://doi.org/10.1007/s11694-021-01228-7>.

**Acknowledgements** This work was supported by the Universidad Autónoma Chapingo [projects 19026-ECI-62, 20225-C-62]; and Consejo Nacional de Ciencia y Tecnología (CONACyT) [Ph.D. scholarship 384708].

**Author contributions** VC-V: conceptualization, formal analysis, investigation, writing—original draft, visualization; LH-R: project administration, funding acquisition, supervision, writing—review and editing; CL-C: resources, funding acquisition, writing—review and editing; JCC-B: writing—review and editing; JA-R: supervision, writing—review and editing; EJV-C: writing—review and editing; BEH-R: writing—review and editing.

**Data availability** All raw data are available from the corresponding author upon reasonable request.

## Declarations

**Conflict of interest** The authors declare no conflict of interest.

## References

- D. Raddatz-Mota, L.J. Pérez-Flores, F. Carrari, J.A. Mendoza-Espinoza, F.D. de León-Sánchez, L.L. Pinzón-López, G. Godoy-Hernández, F. Rivera-Cabrera, *J. Food Sci. Technol.* **54**(6), 1729 (2017)
- H. Ahsan, A. Ahad, J. Iqbal, W.A. Siddiqui, *Nutr. Metab.* **11**(1), 52 (2014)
- M. Viuda-Martos, G.L. Ciro-Gómez, Y. Ruiz-Navajas, J.E. Zapata-Montoya, E. Sendra, J.A. Pérez-Álvarez, J. Fernández-López, *J. Food Saf.* **32**(4), 399–406 (2012)
- J.A. Shilpi, M. Taufiq-Ur-Rahman, S.J. Uddin, M.S. Alam, S.K. Sadhu, V. Seidel, *J. Ethnopharmacol.* **108**(2), 264–271 (2006)
- M.A. Valério, M.I.L. Ramos, J.A. Braga Neto, M.L.R. Macedo, *Food Sci. Technol.* **35**(2), 326–330 (2015)
- E.K. Silva, M. Martelli-Tosi, R. Vardanega, G.C. Nogueira, G.L. Zabet, M.A.A. Meireles, *J. Clean. Prod.* **189**, 231–239 (2018)
- T.M. Garcia Silveira, D.R. Tapia-Blácido, *Food Hydrocoll.* **77**, 117–125 (2018)
- G.L. Zabet, E.K. Silva, L.B. Emerick, M.H.F. Felisberto, M.T.P.S. Clerici, M.A.A. Meireles, *Food Hydrocoll.* **89**, 321–329 (2019)
- J. Ye, X. Hu, S. Luo, D.J. McClements, L. Liang, C. Liu, *Food Res. Int.* **106**, 404–409 (2018)
- Y. Ding, J. Cheng, Q. Lin, Q. Wang, J. Wang, G. Yu, *Food Hydrocoll.* **111**, 106254 (2021)
- M.B. Cardoso, J.-L. Putaux, D. Samios, N.P. da Silveira, *Carbohydr. Polym.* **70**(2), 160–165 (2007)
- Z.H. Lu, E. Donner, Q. Liu, *Starch Stärke* **71**(11–12), 1900123 (2019)
- A.A. Karim, M.Z. Nadiha, F.K. Chen, Y.P. Phuah, Y.M. Chui, A. Fazilah, *Food Hydrocoll.* **22**(6), 1044–1053 (2008)
- M.Z.N. Nadiha, A. Fazilah, R. Bhat, A.A. Karim, *Food Chem.* **121**(4), 1053–1059 (2010)
- C. Lobato-Calleros, C. Ramírez-Santiago, E.J. Vernon-Carter, J. Alvarez-Ramirez, *J. Food Eng.* **131**, 110–115 (2014)
- L. Wang, C. Zhang, Z. Chen, X. Wang, K. Wang, Y. Li, R. Wang, X. Luo, Y. Li, J. Li, *J. Cereal Sci.* **84**, 125–131 (2018)
- D.S. de Castro, I. dos Santos Moreira, L.M. de Melo Silva, J.P. Lima, W.P. da Silva, J.P. Gomes, R.M.F. de Figueirêdo, *Food Res. Int.* **124**, 181–187 (2019)
- R.C.T. Barbi, G.L. Teixeira, P.S. Hornung, S. Ávila, R. Hoffmann-Ribani, *Food Hydrocoll.* **77**, 646–658 (2018)
- J.E. Devia, L. Saldarriaga, *Rev. Univ. EAFIT* **39**(131), 8–22 (2003)
- K. Israkarn, N.N. Nakornpanom, P. Hongprabhas, *Carbohydr. Polym.* **105**, 34–40 (2014)
- AACC, *Approved Methods of Analysis*, 10th edn. (Cereals & Grains Association, St. Paul, 2000)
- T. Zhu, D.S. Jackson, R.L. Wehling, B. Geera, *Cereal Chem. J.* **85**(1), 51–58 (2008)
- R.L. Zapata-Luna, T. Ayora-Talavera, N. Pacheco, E. García-Márquez, H. Espinosa-Andrews, Á. Ku-González, J. Ruiz-Ruiz, J.C. Cuevas-Bernardino, *J. Food Meas. Charact.* **15**(2), 1410–1421 (2021)
- J. Hoyos-Leyva, L.A. Bello-Pérez, E. Agama-Acevedo, J. Alvarez-Ramirez, *Int. J. Biol. Macromol.* **120**, 237–244 (2018)
- A. Milani, M. Jouki, M. Rabbani, *Food Sci. Nutr.* **8**, 3768–3776 (2020)
- S.M.B. Hashemi, D. Jafarpour, *J. Food Sci.* **86**, 513–522 (2021)
- M. Jouki, N. Khazaei, S. Rashidi-Alavijeh, S. Ahmadi, *Food Hydrocoll.* **120**, 106895 (2021)
- D. Gómez-Maldonado, C. Lobato-Calleros, E. Aguirre-Mandujano, S.G. Leyva-Mir, L. Robles-Yerena, E.J. Vernon-Carter, *LWT* **126**, 109337 (2020)
- B.C. Maniglia, D.R. Tapia-Blácido, *Food Hydrocoll.* **55**, 47 (2016)
- S.M.B. Hashemi, D. Jafarpour, *Food Sci. Nutr.* **8**(7), 3128–3137 (2020)
- S.M.B. Hashemi, D. Jafarpour, *J. Food Meas. Charact.* **15**(3), 2516–2523 (2021)
- S.M.B. Hashemi, D. Jafarpour, *J. Food Process. Preserv.* **44**(9), 1–12 (2020)
- M. Jouki, N. Khazaei, F. Rezaei, R. Taghavian-Saeid, *Int. Dairy J.* **122**, 105133 (2021)
- Q.Y. Yang, X.X. Lu, Y.Z. Chen, Z.G. Luo, Z.G. Xiao, *Ultrason. Sonochem.* **51**, 350–358 (2019)
- S. Sukhija, S. Singh, C.S. Riar, *Food Hydrocoll.* **55**, 56–64 (2016)
- S.M. Londoño-Restrepo, N. Rincón-Londoño, M. Contreras-Padilla, A.A. Acosta-Osorio, L.A. Bello-Pérez, J.C. Lucas-Aguirre, V.D. Quintero, P. Pineda-Gómez, A. del Real-López, M.E. Rodríguez-García, *Int. J. Biol. Macromol.* **65**, 222–228 (2014)
- T.Y. Wu, C.R. Chang, T.J. Chang, Y.J. Chang, Y. Liew, C.F. Chau, *Food Chem.* **283**, 46–51 (2019)
- H.N. Englyst, S.M. Kingman, J.H. Cummings, *Eur. J. Clin. Nutr.* **46**(Suppl 2), S33–S50 (1992)
- L.F. Polesi, S.B.S. Sarmiento, S.G. Canniatti-Brazaca, *Rice Sci.* **25**(1), 42–51 (2018)

40. W.R. Morrison, *J. Cereal Sci.* **8**(1), 1–15 (1988)
41. M.R. Debet, M.J. Gidley, *Carbohydr. Polym.* **64**(3), 452–465 (2006)
42. N. Bahrami, L. Yonekura, R. Linforth, M. Carvalho da Silva, S. Hill, S. Penson, G. Chope, I.D. Fisk, *J. Sci. Food Agric.* **94**(3), 415–423 (2014)
43. S. Wang, H. Luo, J. Zhang, Y. Zhang, Z. He, S. Wang, *J. Agric. Food Chem.* **62**(16), 3636–3643 (2014)
44. S. Wang, L. Copeland, *Food Chem.* **135**(3), 1635–1642 (2012)
45. J.Y. Li, A.I. Yeh, *J. Food Eng.* **50**(3), 141–148 (2001)
46. C. Martínez, F. Cuevas, *Evaluación de La Calidad Culinaria y Molinera Del Arroz. Guía de Estudio*, Tercera. (Centro Internacional de Agricultura Tropical (CIAT), Cali, 1989)
47. F.M. Bhat, C.S. Riar, *Int. J. Biol. Macromol.* **92**, 637–644 (2016)
48. C. Cano-Sarmiento, D.I. Téllez-Medina, R. Viveros-Contreras, M. Cornejo-Mazón, C.Y. Figueroa-Hernández, E. García-Armenta, L. Alamilla-Beltrán, H.S. García, G.F. Gutiérrez-López, *Food Eng. Rev.* **10**(3), 113–138 (2018)
49. M.T. Pacheco, F.J. Moreno, R. Moreno, M. Villamiel, O. Hernandez-Hernandez, *Food Chem.* **301**, 125268 (2019)
50. Y. Feng, S.R. Kilker, Y. Lee, in *Charact.*, ed. by S.M. Jafari. Nanoencapsulated Food Ingredients (Academic Press, Gorgan University of Agricultural Sciences and Natural Resources, Gorgan, Iran, 2020), pp. 213–241
51. R.A. Marsh, S.G. Waight, *Starch Stärke* **34**(5), 149–152 (1982)
52. P.P. Rao, G.N. Rao, T. Jyothirmayi, A. Satyanarayana, M.S.L. Karuna, R.B.N. Prasad, *J. Am. Oil Chem. Soc.* **92**(10), 1483–1490 (2015)
53. R. Wongsagonsup, S. Shobsngob, B. Oonkhanond, S. Varavinit, *Starch Stärke* **57**(1), 25–31 (2005)
54. R.G. Utrilla-Coello, M.E. Rodríguez-Huezo, H. Carrillo-Navas, C. Hernández-Jaimes, E.J. Vernon-Carter, J. Alvarez-Ramirez, *Carbohydr. Polym.* **101**(1), 154–162 (2014)
55. R.C. Chisté, A.Z. Mercadante, A. Gomes, E. Fernandes, J.L.F. da Costa Lima, N. Bragagnolo, *Food Chem.* **127**(2), 419–426 (2011)
56. B.A. Acosta-Estrada, J.A. Gutiérrez-Urbe, S.O. Serna-Saldívar, *Food Chem.* **152**, 46–55 (2014)
57. F. Zhu, *Trends Food Sci. Technol.* **43**(1), 1–17 (2015)
58. N.A. Abdul Aziz, L.M. Wong, R. Bhat, L.H. Cheng, *J. Sci. Food Agric.* **92**(3), 557–563 (2012)
59. S. Punia, S.B. Dhull, P. Kunner, S. Rohilla, *Int. J. Biol. Macromol.* **157**, 584–590 (2020)
60. Y. Monroy, S. Rivero, M.A. García, *Ultrason. Sonochem.* **42**, 795–804 (2018)
61. GMd.S. Silva, C.M. Veloso, L.S. Santos, B.A. de Melo Neto, Rd.C.I. Fontan, R.C.F. Bonomo, *J. Food Sci. Technol.* **57**(5), 1830–1839 (2020)
62. F.M. Pelissari, M.M. Andrade-Mahecha, Pjd.A. Sobral, F.C. Menegalli, *Starch Stärke* **64**(5), 382–391 (2012)
63. I. Dankar, A. Haddarah, F.E.L. Omar, M. Pujolà, F. Sepulcre, *Food Chem.* **260**, 7–12 (2018)
64. W. Li, B.J. Dobraszczyk, A. Dias, A.M. Gil, *Cereal Chem. J.* **83**(4), 407–410 (2006)
65. S. Srichuwong, J.-L. Jane, *Food Sci. Biotechnol.* **16**(5), 663–674 (2007)
66. N.W.H. Cheetham, L. Tao, *Carbohydr. Polym.* **36**(4), 277–284 (1998)
67. M.R. Debet, M.J. Gidley, *J. Agric. Food Chem.* **55**(12), 4752–4760 (2007)
68. Z. Li, C. Wei, *Int. J. Biol. Macromol.* **163**, 2084–2096 (2020)
69. J. Alvarez-Ramirez, R. Escarela-Perez, E.J. Vernon-Carter, H. Carrillo-Navas, *J. Cereal Sci.* **88**, 31–37 (2019)
70. X.Z. Han, O.H. Campanella, H. Guan, P.L. Keeling, B.R. Hamaker, *Carbohydr. Polym.* **49**(3), 323–330 (2002)
71. S. Singh, N. Singh, N. Isono, T. Noda, *J. Agric. Food Chem.* **58**, 1180 (2010)
72. S. Takahashi, P.A. Seib, *Cereal Chem.* **65**(6), 474–483 (1988)
73. S. Jitgarmkusol, J. Hongsuwankul, K. Tananuwigong, *Food Chem.* **110**(1), 23–30 (2008)
74. A. Ali, T.A. Wani, I.A. Wani, F.A. Masoodi, *J. Saudi Soc. Agric. Sci.* **15**(1), 75–82 (2016)
75. Z. Sui, T. Yao, X. Ye, J. Bao, X. Kong, Y. Wu, *Starch Stärke* **69**(7–8), 1600164 (2017)
76. L. Lin, C. Cai, R.G. Gilbert, E. Li, J. Wang, C. Wei, *Food Hydrocoll.* **52**, 359–368 (2016)

**Publisher's Note** Springer Nature remains neutral with regard to jurisdictional claims in published maps and institutional affiliations.